SIAM J. NUMER. ANAL.
Vol. 0, No. 0, pp. 000–000 

# DISCONTINUOUS GALERKIN METHODS FOR NONLINEAR SCALAR CONSERVATION LAWS: GENERALIZED LOCAL LAX–FRIEDRICHS NUMERICAL FLUXES*

JIA LI†, DAZHI ZHANG†, XIONG MENG‡, BOYING WU†, AND QIANG ZHANG§

**Abstract.** In this paper, we study the discontinuous Galerkin method with a class of generalized numerical fluxes for one-dimensional scalar nonlinear conservation laws. The generalized local Lax–Friedrichs (GLLF) fluxes with two weights, which may not be monotone, are proposed and analyzed. Under a condition for the weights, we first show the monotonicity for the flux and thus the $L^2$ stability of the scheme. Then, by constructing and analyzing a special piecewise global projection which commutes with the time derivative operator, we are able to show optimal error estimates for the DG scheme with GLLF fluxes. The result is sharp for monotone numerical fluxes, for which only suboptimal estimates can be proved in previous work. Moreover, optimal error estimates are still valid for fluxes that are not monotone, allowing us to choose some suitable weights to achieve less numerical dissipation and thus to better resolve shocks. Numerical experiments are provided to show the sharpness of theoretical results.

**Key words.** nonlinear conservation laws, discontinuous Galerkin methods, generalized local Lax–Friedrichs fluxes, optimal error estimates

**AMS subject classifications.** 65M12, 65M15, 65M60

**DOI.** 10.1137/19M1243798

## 1. Introduction.

In this paper, we concentrate on discontinuous Galerkin (DG) methods with generalized local Lax–Friedrichs (GLLF) fluxes for one-dimensional scalar nonlinear hyperbolic conservation laws

$$u_t + f(u)_x = 0, \qquad (x,t) \in I \times (0,T], \tag{1.1a}$$

$$u(x,0) = u_0(x), \qquad x \in I, \tag{1.1b}$$

where $u_0(x)$ is a smooth function and $I = [a,b]$. The nonlinear function $f(u)$ is assumed to be sufficiently smooth with respect to $u$. Note that the GLLF flux is in a more general setting of the local Lax–Friedrichs (LLF) flux, which is not even *monotone* and can be regarded as an extension of upwind-biased fluxes when $f(u)$ is linear [20]. The $L^2$ stability and optimal error estimates are obtained for the GLLF fluxes with two suitable weights. The periodic boundary conditions are considered.

The DG method discussed in this paper is a class of finite element methods, which was first introduced by Reed and Hill [23] for solving a steady-state linear hyperbolic

*Received by the editors February 11, 2019; accepted for publication (in revised form) October 29, 2019; published electronically DATE.
https://doi.org/10.1137/19M1243798
**Funding:** The work of the first and third authors was supported by National Natural Science Foundation of China grant 11501149. The work of the second author was supported by National Key Research and Development Program in China grant 2017YFB1401801 and National Natural Science Foundation of China grant 71773024. The work of the fifth author was supported by National Natural Science Foundation of China grants 11671199 and 11571290.

†School of Mathematics, Harbin Institute of Technology, Harbin 150001, Heilongjiang, China (jli@hit.edu.cn, zhangdazhi@hit.edu.cn, mathwby@hit.edu.cn).
‡Corresponding author. School of Mathematics and Institute for Advanced Study in Mathematics, Harbin Institute of Technology, Harbin 150001, Heilongjiang, China (xiongmeng@hit.edu.cn).
§Department of Mathematics, Nanjing University, Nanjing 210093, Jiangsu, China (qzh@nju.edu.cn).

equation and was developed by Cockburn and Shu [12] for time-dependent nonlinear conservation laws. For the time discretization, the explicit total variation diminishing (TVD) Runge–Kutta method [15] is usually adopted. We refer to the survey paper [25] for recent development of DG methods for time-dependent problems.

As is well known, the numerical flux is the most important ingredient in designing DG schemes, since it determines many features of DG methods such as the stability and accuracy. Typically, for nonlinear scalar conservation laws, the numerical fluxes are chosen as *monotone* fluxes, and $L^2$ stability [16] and a suboptimal error estimate of order $k+\frac{1}{2}$ are obtained for the fully discrete scheme combined with third order TVD Runge–Kutta methods in [26]. Moreover, when upwind numerical flux is used, the optimal error estimate of order $k+1$ is proved [26]. For general stabilized finite element methods for linear symmetric hyperbolic systems, a suboptimal error estimate of order $k+\frac{1}{2}$ is obtained for the space-time methods [13] and for the Runge–Kutta DG methods [4]. Throughout the paper, $k$ is the highest polynomial degree of the discontinuous finite element space.

To provide more flexibility in numerical viscosity with potential applications to complex systems, the numerical fluxes are recently chosen in a general pattern. Specifically, for DG approximation to linear spatial derivative terms, some generalized numerical fluxes containing one weight are used. For example, the upwind-biased fluxes are considered for linear hyperbolic equations [20], and the central flux for nonlinear convection term in combination with generalized alternating fluxes for linear diffusion term are used for the Burgers–Poisson equation [18]. Moreover, the generalized numerical fluxes with two independent weights are given in [9] for solving linear convection-diffusion equations. It is worth emphasizing that, for generalized numerical fluxes, optimal error estimates can be derived by virtue of some special *global* projections, which is motivated by the work of [2]. There is some other work related to DG methods with generalized fluxes; see, for example, superconvergence of DG methods with upwind-biased fluxes for one-dimensional linear hyperbolic equations [5], and the local error estimate of local DG methods with generalized alternating fluxes for singularly perturbed problems [10]. In addition, motivated by [1], a class of $\alpha\beta$-fluxes can be proved to be of order $k+1$ for one-dimensional two-way wave equations in [8] and for linear high order equations in [14] by constructing some *local* and *global* projections. The generalized numerical fluxes for direct DG methods for diffusion problems can be found in [7, 19].

How to extend the optimal error analysis of generalized numerical fluxes from linear derivative terms to nonlinear ones is of current interest. It thus would be meaningful to investigate a class of generalized fluxes for nonlinear conservation laws in terms of the GLLF flux, which is a modification of LLF fluxes with two weights representing different numerical viscosities; see (2.2a) and (2.2b) below. Following the idea of *piecewise global* projections for degenerate variable coefficient hyperbolic equations in [17], to minimize the leading term of projection error terms for nonlinear conservation laws we construct a special *piecewise global* projection depending only on two weights and $u$. The resulting projection is a linear operator for $u$ and thus commutes with the time derivative operator. Although the wind direction can be changed, the *piecewise global* projection allows us to establish the optimal approximation property and we need only to pay attention to regions with fixed wind direction, as in the cell on which $f'(u)$ does change its sign, $f'(u)$ itself is of order $h$. Therefore, by a linearization approach for nonlinear flux functions [26, 21], optimal error estimates are obtained for GLLF fluxes.

To the best of our knowledge, this is the first proof of optimal error estimates of the DG scheme with LLF type and generalized numerical flux when nonlinear conservation laws are considered. In this work, the theoretical results not only provide a sharp error estimate for *monotone* fluxes but also establish optimal error estimates for fluxes that are not *monotone*. In addition to the improvement of theoretical analysis, the GLLF flux contributes a lot in practical computation for its better solution in resolving shocks (see Example 4.1).

The organization of this paper is as follows. In section 2, the DG scheme with GLLF fluxes for one-dimensional nonlinear scalar conservation laws is presented and the monotonicity is discussed. In section 3, by designing and analyzing a special *piecewise global* projection, optimal error estimates are obtained under the condition $\lambda > |\theta|$. In section 4, numerical experiments are shown, which confirm the sharpness of optimal error estimates and verify the numerical stability of the DG scheme with *nonmonotone* GLLF fluxes. Concluding remarks are given in section 5.

## 2. The DG scheme with GLLF fluxes.

Let us start by presenting some notation for the mesh, function space, and norms.

### 2.1. Basic notation.

The usual notation of DG methods is adopted. The computational interval $I = [a, b]$ is divided into $N$ cells $I_j = (x_{j-\frac{1}{2}}, x_{j+\frac{1}{2}})$ for $j = 1, \dots, N$, where $a = x_{\frac{1}{2}} < x_{\frac{3}{2}} < \cdots < x_{N+\frac{1}{2}} = b$ and cell center is $x_j = \frac{1}{2}(x_{j-\frac{1}{2}} + x_{j+\frac{1}{2}})$, and the tessellation of $I$ is denoted as $\mathcal{I}_h = \{I_j\}_{j=1}^N$. Denote by $h_j = x_{j+\frac{1}{2}} - x_{j-\frac{1}{2}}$ the mesh size with $h = \max_j h_j$. $\mathcal{I}_h$ is assumed to be quasi-uniform in the sense that there holds $\nu h \le h_j \le h$ $(j = 1, \dots, N)$ for a fixed positive constant $\nu$, as $h$ goes to zero.

The discontinuous finite element space is chosen as

$$V_h^k = \{\omega : \omega|_{I_j} \in P^k(I_j),\ j = 1, \dots, N\},$$

where $P^k(I_j)$ is the space of polynomials of degree up to $k$ on $I_j$. Since $\omega \in V_h^k$ can be discontinuous at cell interfaces, we denote by $\omega^-_{j+\frac{1}{2}}$ and $\omega^+_{j+\frac{1}{2}}$ the values of $\omega$ at $x_{j+\frac{1}{2}}$ from the left cell $I_j$ and the right cell $I_{j+1}$, respectively. Further, the jump and the mean value of $\omega$ at cell boundaries are denoted as $[\![\omega]\!] = \omega^+ - \omega^-$ and $\{\!\{\omega\}\!\} = \frac{1}{2}(\omega^+ + \omega^-)$.

We use $W^{\ell,p}(\Omega)$ (e.g., $\Omega = I_j$) to represent the standard Sobolev space on $\Omega$ equipped with norm $\|\cdot\|_{W^{\ell,p}(\Omega)}$, where $\ell \ge 0,\ 1 \le p \le \infty$ are integers. Then the *broken* Sobolev space on $\mathcal{I}_h$ is denoted as

$$W^{\ell,p}(\mathcal{I}_h) = \{u \in L^2(I) : u|_{I_j} \in W^{\ell,p}(I_j),\ j = 1, \dots, N\},$$

and the norms are denoted as $\|u\|_{W^{\ell,\infty}(\mathcal{I}_h)} = \max_{1\le j\le N} \|u\|_{W^{\ell,\infty}(I_j)}$, $\|u\|_{W^{\ell,p}(\mathcal{I}_h)} = (\sum_{j=1}^N \|u\|^p_{W^{\ell,p}(I_j)})^{1/p}$ for $p \ne \infty$. The notation $H^\ell(\mathcal{I}_h) = W^{\ell,2}(\mathcal{I}_h)$, $L^2(I) = H^0(\mathcal{I}_h)$, and $L^\infty(I) = W^{0,\infty}(\mathcal{I}_h)$ is adopted. In addition, the boundary norms are denoted as $\|u\|^2_{L^2(\Gamma_h)} = \sum_{j=1}^N \|u\|^2_{L^2(\partial I_j)}$ and $\|u\|^2_{L^2(\partial I_j)} = (u^+_{j-\frac{1}{2}})^2 + (u^-_{j+\frac{1}{2}})^2$.

### 2.2. The DG scheme.

For nonlinear conservation laws (1.1), the DG scheme is as follows: $\forall t \in (0, T]$, find $u_h(t) \in V_h^k$ such that for any $v_h \in V_h^k$ and $j = 1, \dots, N$ there holds

$$\int_{I_j} (u_h)_t v_h \mathrm{d}x - \int_{I_j} f(u_h)(v_h)_x \mathrm{d}x + \hat{f}_{j+\frac{1}{2}}(v_h)^-_{j+\frac{1}{2}} - \hat{f}_{j+\frac{1}{2}}(v_h)^+_{j-\frac{1}{2}} = 0. \tag{2.1}$$

Instead of using *monotone* fluxes, we consider the following GLLF fluxes that may not be *monotone*

(2.2a)
$$\hat{f}(u_h^-,u_h^+) = \left(\frac{1}{2}+\theta\right) f(u_h^-) + \left(\frac{1}{2}-\theta\right) f(u_h^+) - \lambda\alpha(u_h^+ - u_h^-),\ \ \alpha = \max_{\omega\in[c,d]} |f'(\omega)|,$$

where $c = \min(u_h^-,u_h^+), d = \max(u_h^-,u_h^+)$, and $\theta$, $\lambda$ are two weights satisfying

$$\lambda > |\theta|, \tag{2.2b}$$

which comes from the application of flux (2.2a) to linear hyperbolic equations with upwind-biased numerical fluxes. Note that (2.2b) will guarantee provable linear stability for the GLLF fluxes as well as uniqueness existence of the newly designed projection in (3.1) and thus optimal error estimates; for more details, see Remark 3.4. Indeed, the flux (2.2a) and (2.2b) will reduce to the upwind-biased fluxes [20] when $f$ is linear and the standard LLF flux when $\theta = 0,\ \lambda = \frac{1}{2}$. Moreover, the weights $\theta$ and $\lambda$ are chosen based on a balance of numerical viscosity between an E-flux [22] and the central flux, since, as shown in (3.18) below, the numerical viscosity coefficient is $\theta f'(u)+\lambda\alpha$ depending on $\lambda$ and $\theta$. Specifically, the adjustable coefficient is $\theta f'(u)+\lambda\alpha$ and will be close to that of an E-flux, which is beneficial for shocks (bigger $\lambda - |\theta|$), and to that of the central flux, which is useful for smooth solutions (smaller $\lambda - |\theta|$).

**2.3. Monotonicity of the GLLF flux.** Note that the nonlinear $L^2$ stability property cannot be proved for the DG scheme with (2.2b), although it is numerically stable. A rigorous proof of the $L^2$ stability for GLLF fluxes with (2.2b) is more involved and will be studied in future work. Therefore, following [16], a much stronger condition is proposed which will lead to the monotonicity of the GLLF flux and thus $L^2$ stability.

LEMMA 2.1. *The GLLF flux* (2.2) *is monotone if*

$$\lambda \geq \frac{1}{2} + |\theta|. \tag{2.3}$$

*Proof.* It suffices to show that $\hat{f}$ is a nondecreasing function of its first argument and a nonincreasing function of its second argument in the sense that for $\forall\omega \in [\min(u_h^-,u_h^+), \max(u_h^-,u_h^+)]$, $\hat{f}(\omega,u_h^+) - \hat{f}(u_h^-,u_h^+) \geq 0$ and $\hat{f}(u_h^-,u_h^+) - \hat{f}(u_h^-,\omega) \leq 0$.

Without loss of generality, we assume $u_h^- < u_h^+$. If $\omega = u_h^-$, then $\hat{f}(\omega,u_h^+) - \hat{f}(u_h^-,u_h^+) = 0$. If $\forall\omega \in (u_h^-,u_h^+]$, there holds $\omega - u_h^- > 0$, and we divide $\hat{f}(\omega,u_h^+) - \hat{f}(u_h^-,u_h^+)$ by $\omega - u_h^-$ to obtain

$$\frac{\hat{f}(\omega,u_h^+) - \hat{f}(u_h^-,u_h^+)}{\omega - u_h^-} = \left(\frac{1}{2}+\theta\right)\frac{f(\omega)-f(u_h^-)}{\omega - u_h^-} + \lambda\alpha. \tag{2.4}$$

By the mean value theorem and the definition of $\alpha$, one has

$$\Big|\frac{f(\omega)-f(u_h^-)}{\omega - u_h^-}\Big| \leq \alpha.$$

Thus, a substitution of the above estimate, the fact that $\omega - u_h^- > 0$, and the condition $\lambda \geq \frac{1}{2} + |\theta|$ into (2.4) lead to the desired result,

$$\hat{f}(\omega,u_h^+) - \hat{f}(u_h^-,u_h^+) \geq 0.$$

Analogously, we can also prove $\hat{f}(u_h^-, u_h^+) - \hat{f}(u_h^-, \omega) \leq 0$. Therefore, the GLLF flux (2.2) with (2.3) is *monotone*. ◻

Monotonicity of the numerical flux (2.2a) with (2.3) would lead to $L^2$ stability of the DG scheme [16, 24].

PROPOSITION 2.2. *The DG scheme with flux* (2.2a) *and* (2.3) *is $L^2$ stable.*

## 3. Optimal error estimates.

This section is devoted to the analysis of optimal error estimates of DG methods with GLLF fluxes (2.2) for nonlinear conservation laws. We begin by presenting some preliminary results on projections and inverse properties that will be used later.

### 3.1. Preliminaries.

#### 3.1.1. Projections.

It is well known that design and analysis of some special projections are essential in deriving optimal error estimates, especially when generalized numerical fluxes are considered. In particular, when generalized fluxes are used for nonlinear equations, the following three properties should be taken into account when designing projections.

The first one is that the projection should eliminate terms involving projection errors as much as possible, namely to minimize the contribution of projection terms. This can be achieved by requiring the projection errors to be orthogonal to polynomials of degree up to $k-1$ and an exact collocation of the projection error at cell boundaries. For example, when upwind flux is applied, the locally defined Gauss–Radau (GR) projection can totally eliminate projection errors on the boundaries [6, 2]. When generalized fluxes are used, the collocation requirement would make projection *global* (e.g., [20, 18]) and also eliminate projection errors at boundaries.

The second one is that the unique existence and optimal approximation properties of the resulting projection are provable, which can be accomplished by analyzing a *global* projection [20, 9] for generalized fluxes when the wind direction does not change. However, when wind direction does change, existence and uniqueness of the projection cannot be established if simply constructing a *global* projection as before. Instead, the idea of introducing a *piecewise global* projection for different regions on which the wind direction keeps its sign is essential; see, e.g., [17], in which degenerate linear variable coefficient hyperbolic equations with upwind-biased fluxes are considered.

The last one is that the projection should be linear of $u$ without any time variable explicitly involved, so that the estimate to the time derivative of projection error is a trivial consequence of that of the projection error itself. In particular, the standard *local* GR projection naturally satisfies this property [6], and when generalized fluxes are adopted, this property also holds by defining projections to be dependent only on some weights but not on $u$ [18, 20, 9, 17]. It is this property that we only consider the leading term of projection errors, and we fully make use of the relation that, at $x_{j+\frac{1}{2}}$, $\alpha = |f'(u_{j+\frac{1}{2}})| + \mathcal{O}(h)$, which is valid for LLF type fluxes.

We are now ready to present the definition of a *piecewise global* projection that is linear for $u$ and also for the time derivative operator. To do that, we first assume $f'(u)$ has finite zeros on $I$. As $h$ goes to zero, we can assume there exists at most one zero on any cell $I_j$ for $j = 1, \dots, N$. Indeed, the zeros of $f'(u)$ do not vary with respect to the time variable $t$, since the exact solution is assumed to be smooth and thus $f'(u(x,t)) = f'(u_0(x))$, which is quite beneficial for us to construct a satisfactory projection. To clearly display the main idea in designing a *piecewise global* projection satisfying the three properties mentioned, let us mainly consider the case that $f'(u)$ has only two zeros: the case with more zeros can be defined by combining [17] and the technique discussed in this paper. We adopt the notation $\mathbb{Z}_N^+ = \{1, 2, \ldots, N\}$ and define $\gamma, \beta \in \mathbb{Z}_N^+$ as

$$\gamma = \{j \;\big|f'(u_{j-\frac{1}{2}}) > 0 \text{ and } f'(u_{j+\frac{1}{2}}) \le 0 \;\; \forall j \in \mathbb{Z}_N^+\},$$

$$\beta = \{j \;\big|f'(u_{j-\frac{1}{2}}) < 0 \text{ and } f'(u_{j+\frac{1}{2}}) \ge 0 \;\; \forall j \in \mathbb{Z}_N^+\}.$$

Note that $\gamma$ and $\beta$ are two fixed numbers determined by $f'(u_0(x))$; for more details, see [17]. Similar to [17, section 3.1], we can use a unified notation for two index sets

$$\mathbb{b}^+ = \{\beta, \ldots, \gamma - 1\}, \quad \mathbb{b}^- = \{\gamma + 1, \ldots, \beta - 1\},$$

for periodic boundary conditions, no matter which ($\gamma$ or $\beta$) is bigger.

Then the *piecewise global* projection, denoted by $\mathcal{P}_h u$, is defined as follows: for $u \in H^1(\mathcal{I}_h)$, we define the projection $\mathcal{P}_h u \in V_h^k$ satisfying

$$\int_{I_j} (\mathcal{P}_h u)\varphi \mathrm{d}x = \int_{I_j} u\varphi \mathrm{d}x \qquad \forall \varphi \in P^{k-1}(I_j), \qquad j \in \mathbb{Z}_N^+, \tag{3.1a}$$

$$(\mathcal{P}_h u)^-_{j+\frac{1}{2}} = u^-_{j+\frac{1}{2}} \qquad \text{at } x_{j+\frac{1}{2}}, \qquad j = \gamma, \tag{3.1b}$$

$$(\widehat{\mathcal{P}_h u}^{\,p})_{j+\frac{1}{2}} = \hat{u}^p_{j+\frac{1}{2}} \qquad \text{at } x_{j+\frac{1}{2}}, \qquad j \in \mathbb{b}^+, \tag{3.1c}$$

$$(\widehat{\mathcal{P}_h u}^{\,n})_{j-\frac{1}{2}} = \hat{u}^n_{j-\frac{1}{2}} \qquad \text{at } x_{j-\frac{1}{2}}, \qquad j \in \mathbb{b}^-, \tag{3.1d}$$

where the superscript $p$ ($n$) refers to the index set of a region on which $f'(u_{j+\frac{1}{2}})$ is positive (negative), and $\forall z \in H^1(\mathcal{I}_h)$

$$\hat{z}^p = \left(\frac{1}{2} + (\lambda+\theta)\right) z^- + \left(\frac{1}{2} - (\lambda+\theta)\right) z^+, \; \hat{z}^n = \left(\frac{1}{2} - (\lambda-\theta)\right) z^- + \left(\frac{1}{2} + (\lambda-\theta)\right) z^+.$$

*Remark* 3.1. The *piecewise global* projection (3.1) defines a stronger (local) collocation at $x_{\gamma+\frac{1}{2}}$. Moreover, a combination of (3.1d) with (3.1b) will lead to an inherent local collocation at $x_{\gamma+\frac{1}{2}}$, namely

$$(\mathcal{P}_h u)^+_{j-\frac{1}{2}} = u^+_{j-\frac{1}{2}}, \quad j = \gamma + 1.$$

Therefore, the projection (3.1) can be decoupled starting from $I_\gamma$ or $I_{\gamma+1}$, and this is why it is called a *piecewise global* projection. Note that when $f'(u(x,t))$ does not change its sign $\forall (x,t) \in I \times (0,T]$, the *piecewise global* projection defined above will reduce to some *global* projections as those in [20, 9].

The optimal approximation property of $\mathcal{P}_h u$ is given in the following lemma.

LEMMA 3.2. *Assume $u$ is smooth and periodic, and $f'(u)$ has finite zeros on $I$; then there exists a unique projection $\mathcal{P}_h u$ satisfying* (3.1)*. Moreover, there holds the following optimal approximation property:*

$$\|u - \mathcal{P}_h u\|_{L^2(I)} + h^{\frac{1}{2}} \|u - \mathcal{P}_h u\|_{L^2(\Gamma_h)} \le C h^{k+1} \|u\|_{H^{k+1}(\mathcal{I}_h)}, \tag{3.2}$$

*where $C$ is independent of the mesh size $h$.*

The proof of Lemma 3.2 is postponed to the appendix.

As for the initial discretization, we would like to use the standard $L^2$ projection $\pi_h$, and we have

$$\|u_0 - \pi_h u_0\|_{L^2(I)} \le C h^{k+1} \|u_0\|_{H^{k+1}(\mathcal{I}_h)}. \tag{3.3}$$

**3.1.2. Inverse inequalities and the a priori assumption.** The following inverse properties [3, 11] will be used for nonlinear equations. For all $v_h \in V_h^k$, there holds (i) $\|(v_h)_x\|_{L^2(I)} \leq Ch^{-1}\|v_h\|_{L^2(I)}$, (ii) $\|v_h\|_{L^2(\Gamma_h)} \leq Ch^{-\frac{1}{2}}\|v_h\|_{L^2(I)}$, (iii) $\|v_h\|_{L^\infty(I)} \leq Ch^{-\frac{1}{2}}\|v_h\|_{L^2(I)}$.

Denoting the error as $e = u - u_h$ and $\eta = u - \mathcal{P}_h u$, $\xi = \mathcal{P}_h u - u_h$, the following a priori assumption is useful to deal with high order terms

$$\|\xi(t)\|_{L^2(I)} \leq h^{\frac{3}{2}} \quad \forall t \in (0,T]. \tag{3.4}$$

By the triangle inequality, (3.4), and inverse property (iii), it is easy to show for $k \geq 1$

$$\|e(t)\|_{L^\infty(I)} \leq \|\eta(t)\|_{L^\infty(I)} + \|\xi(t)\|_{L^\infty(I)} \leq Ch \quad \forall t \in (0,T], \tag{3.5}$$

where we have also used the estimate $\|\eta(t)\|_{L^\infty(I)} \leq Ch^{k+\frac{1}{2}}$ implied by (3.2) and the Sobolev inequality. The a priori assumption (3.4) can be verified by the continuity of $\|\xi(t)\|$ and optimal error estimate in (3.6) below, with the initial error estimate at $t = 0$ as a starting point; for more details, we refer to [21].

**3.2. The main result.** We are now ready to state the optimal error estimates, which hold for GLLF fluxes that are not even *monotone*, as long as (2.2b) is satisfied.

THEOREM 3.3. *Let $u$ be the exact solution of* (1.1)*, which is assumed to be sufficiently smooth, i.e., $\|u\|_{H^{k+1}(\mathcal{I}_h)}$ and $\|u_t\|_{H^{k+1}(\mathcal{I}_h)}$ are bounded uniformly for any time $t \in [0,T]$. Assume $f$ is smooth, for example, $f \in C^2$. Let $u_h$ be the DG solution with GLLF fluxes* (2.2) *for solving nonlinear conservation laws. If piecewise polynomials space $V_h^k$ of degree $k \geq 1$ is used, then for small enough $h$ there holds the following optimal error estimate:*

$$\|u(t) - u_h(t)\|_{L^2(I)} \leq Ch^{k+1} \quad \forall t \in (0,T], \tag{3.6}$$

*where $C$ is independent of $h$.*

**3.3. Proof of the main result.** We will finish the proof with the following five steps.

**Step 1: Error equation and error decomposition.** Since the exact solution $u$ also satisfies the DG scheme (2.1), by Galerkin orthogonality, there holds the cell error equation

$$\int_{I_j} e_t v_h \mathrm{d}x = \int_{I_j} \big(f(u) - f(u_h)\big)(v_h)_x \mathrm{d}x - (f - \hat{f})v_h^-\big|_{j+\frac{1}{2}} + (f - \hat{f})v_h^+\big|_{j-\frac{1}{2}} \tag{3.7}$$

for any $v_h \in V_h^k$ and $j = 1, \ldots, N$, where $e = u - u_h$. Typically, to deal with nonlinear flux functions, the following linearization technique based on Taylor expansion should be used.

On any cell $I_j$, by the second order Taylor expansion, one has

$$f(u) - f(u_h) = f'(u)e - R_0 e^2,$$

where $R_0 = \frac{1}{2}\int_0^1 f''(u + s(u_h - u))(1 - s)\mathrm{d}s$. Next, to deal with nonlinear boundary terms, namely $f(u_{j+\frac{1}{2}}) - \hat{f}((u_h^-)_{j+\frac{1}{2}}, (u_h^+)_{j+\frac{1}{2}})$, we need to apply the second order Taylor expansion to each nonlinear term in the GLLF flux (2.2); when omitting the subscript $j+\frac{1}{2}$, it reads

$$f(u_h^-) = f(u) - f'(u)e^- + R_1(e^-)^2, \quad f(u_h^+) = f(u) - f'(u)e^+ + R_2(e^+)^2,$$

where $R_1 = \frac{1}{2}\int_0^1 f''(u + s(u_h^- - u))(1-s)\mathrm{d}s$, $R_2 = \frac{1}{2}\int_0^1 f''(u + s(u_h^+ - u))(1-s)\mathrm{d}s$. Therefore, at each boundary point $x_{j+\frac{1}{2}}$, by $[\![u_h]\!] = [\![u_h - u]\!] = -[\![\eta]\!] - [\![\xi]\!]$ since $u$ is continuous across cell interfaces, one has, after some simple algebraic calculations

$$f(u) - \hat{f}(u_h^-, u_h^+) = \widehat{f'\eta}^{\,\mathrm{lin}} + \widehat{f'\xi}^{\,\mathrm{lin}} - \widehat{Re^2}^{\,\mathrm{nlr}},$$

where

$$\widehat{f'\eta}^{\,\mathrm{lin}} = \left(\left(\frac{1}{2}+\theta\right) f'(u) + \lambda\alpha\right)\eta^- + \left(\left(\frac{1}{2}-\theta\right) f'(u) - \lambda\alpha\right)\eta^+, \tag{3.8a}$$

$$\widehat{f'\xi}^{\,\mathrm{lin}} = \left(\left(\frac{1}{2}+\theta\right) f'(u) + \lambda\alpha\right)\xi^- + \left(\left(\frac{1}{2}-\theta\right) f'(u) - \lambda\alpha\right)\xi^+, \tag{3.8b}$$

$$\widehat{Re^2}^{\,\mathrm{nlr}} = \left(\frac{1}{2}+\theta\right) R_1(e^-)^2 + \left(\frac{1}{2}-\theta\right) R_2(e^+)^2. \tag{3.8c}$$

For notational convenience, we use the following DG spatial discretization operator: $\forall \rho, \phi \in H^1(\mathcal{I}_h)$,

$$\mathcal{H}_j(\rho, \phi; \hat{\rho}) = \int_{I_j} \rho\phi_x \mathrm{d}x - \hat{\rho}\phi^-\big|_{j+\frac{1}{2}} + \hat{\rho}\phi^+\big|_{j-\frac{1}{2}},$$

and $\mathcal{H}(\rho, \phi; \hat{\rho}) = \sum_{j=1}^N \mathcal{H}_j(\rho, \phi; \hat{\rho})$. Taking $v_h = \xi$ in (3.7) and summing up over all $j$, the error equation can be written as

$$\frac{1}{2}\frac{\mathrm{d}}{\mathrm{d}t}\|\xi\|^2_{L^2(I)} + \int_I \eta_t\xi\mathrm{d}x = \mathcal{H}(f'(u)\eta, \xi; \widehat{f'\eta}^{\,\mathrm{lin}}) + \mathcal{H}(f'(u)\xi, \xi; \widehat{f'\xi}^{\,\mathrm{lin}}) - \mathcal{H}(R_0e^2, \xi; \widehat{Re^2}^{\,\mathrm{nlr}}), \tag{3.9}$$

where $\int_I \eta_t\xi\mathrm{d}x = \sum_{j=1}^N \int_{I_j}\eta_t\xi\mathrm{d}x$. The components on the right-hand side of (3.9) are referred to as "$\eta$ terms," "$\xi$ terms," and "higher order terms," which are estimated in the subsequent three steps.

**Step 2: Estimate of $\boldsymbol{\eta}$ terms.** Note that

$$\mathcal{H}(f'(u)\eta, \xi; \widehat{f'\eta}^{\,\mathrm{lin}}) = \sum_{j=1}^N \int_{I_j} f'(u)\eta\xi_x\mathrm{d}x + \sum_{j=1}^N \left(\widehat{f'\eta}^{\,\mathrm{lin}}[\![\xi]\!]\right)_{j+\frac{1}{2}} \triangleq S_1 + S_2. \tag{3.10}$$

The estimate of $S_1$ can be obtained by using the local linearization $f'(u) = f'(u_j) + f'(u) - f'(u_j)$ and the orthogonality property of $\mathcal{P}_h$ in (3.1a); it reads

$$\begin{aligned} S_1 &= \sum_{j=1}^N \int_{I_j} \big(f'(u_j) + f'(u) - f'(u_j)\big)\eta\xi_x\mathrm{d}x \\ &\le Ch\|\eta\|_{L^2(I)}\|\xi_x\|_{L^2(I)} \le C\|\eta\|_{L^2(I)}\|\xi\|_{L^2(I)} \le Ch^{k+1}\|\xi\|_{L^2(I)}, \end{aligned} \tag{3.11}$$

where we have also used the inverse property (i) and the fact that $|f'(u) - f'(u_j)| \le Ch$ implied by smoothness of $f$ and $u$.

We now turn to the estimate of $S_2$. If we simply define a projection by asking for $\widehat{f'\eta}^{\text{lin}} = 0$ at each cell interface except at $x_{\beta-\frac{1}{2}}$, namely

$$\widehat{f'\eta}^{\text{lin}} = \left(\left(\frac{1}{2}+\theta\right)f'(u)+\lambda\alpha\right)\eta^- + \left(\left(\frac{1}{2}-\theta\right)f'(u)-\lambda\alpha\right)\eta^+ \tag{3.12}$$

to be zero except at $x_{\beta-\frac{1}{2}}$, we can see that the proposed projection would be dependent on $f'(u)$ as well as $\alpha$ and thus on $t$, indicating that it is almost impossible to prove $(\mathcal{P}_h u)_t = \mathcal{P}_h(u_t)$ which will be used to estimate $\|\eta_t\|_{L^2(I)}$.

Fortunately, since $\alpha$ is chosen locally for values between $u_h^-$ and $u_h^+$ at each cell interface for the GLLF flux, it follows from the smoothness of $f$ and $u$ that

$$\alpha = \max_{\omega\in[c,d]} |f'(\omega)| = |f'(u)| + \varepsilon, \quad \text{at } x_{j+\frac{1}{2}}, \tag{3.13}$$

where $|\varepsilon| \le C\|e\|_{L^\infty(I)} \le Ch$ by the estimate (3.5) implied by (3.4). At each cell interface $x_{j+\frac{1}{2}}$, a substitution of (3.13) into (3.12) leads to

$$\widehat{f'\eta}^{\text{lin}} = \left(\left(\frac{1}{2}+\lambda+\theta\right)f'(u)+\lambda\varepsilon\right)\eta^- + \left(\left(\frac{1}{2}-\lambda-\theta\right)f'(u)-\lambda\varepsilon\right)\eta^+, \quad f'(u)>0,$$
$$\widehat{f'\eta}^{\text{lin}} = \left(\left(\frac{1}{2}-\lambda+\theta\right)f'(u)+\lambda\varepsilon\right)\eta^- + \left(\left(\frac{1}{2}+\lambda-\theta\right)f'(u)-\lambda\varepsilon\right)\eta^+, \quad f'(u)\le 0,$$

which is

$$\widehat{f'\eta}^{\text{lin}} = f'(u)\left(\left(\frac{1}{2}+(\lambda+\theta)\right)\eta^- + \left(\frac{1}{2}-(\lambda+\theta)\right)\eta^+\right) - \lambda\varepsilon[\![\eta]\!], \quad f'(u)>0, \tag{3.14a}$$

$$\widehat{f'\eta}^{\text{lin}} = f'(u)\left(\left(\frac{1}{2}-(\lambda-\theta)\right)\eta^- + \left(\frac{1}{2}+(\lambda-\theta)\right)\eta^+\right) - \lambda\varepsilon[\![\eta]\!], \quad f'(u)\le 0, \tag{3.14b}$$

at the cell boundaries $x_{j+\frac{1}{2}}$. By the definition of the special *piecewise global* projection $\mathcal{P}_h$ in (3.1), the first term on the right side of (3.14a) and (3.14b) will be zero except at the point $x_{\beta-\frac{1}{2}}$, namely $f'(u_{\beta-\frac{1}{2}})\hat{\eta}^n_{\beta-\frac{1}{2}} \ne 0$. Consequently, for any $j = 1,\ldots,N$

$$\left|\widehat{f'\eta}^{\text{lin}}_{j+\frac{1}{2}}\right| \le Ch(\|\eta\|_{L^2(\partial I_{\beta-1})} + \|\eta\|_{L^2(\partial I_\beta)} + \|\eta\|_{L^2(\partial I_j)} + \|\eta\|_{L^2(\partial I_{j+1})}),$$

since $|f'(u_{\beta-\frac{1}{2}})| \le Ch$ and $|\varepsilon| \le Ch$. Then the Cauchy–Schwarz inequality, inverse inequality (ii), and optimal approximation property (3.2) give us a bound of $S_2$,

$$S_2 \le Ch\|\eta\|_{L^2(\Gamma_h)}\|\xi\|_{L^2(\Gamma_h)} \le Ch^{k+1}\|\xi\|_{L^2(I)}. \tag{3.15}$$

A combination of (3.11) and (3.15) leads to the estimate to $\eta$ terms

$$\mathcal{H}(f'(u)\eta, \xi; \widehat{f'\eta}^{\text{lin}}) \le Ch^{k+1}\|\xi\|_{L^2(I)}, \tag{3.16}$$

where $C$ is independent of $h$.

**Step 3: Estimate of $\boldsymbol{\xi}$ terms.** Using integration by parts, we have

$$
\begin{aligned}
&\mathcal{H}(f'(u)\xi, \xi; \widehat{f'\xi}^{\,\mathrm{lin}})\\
&= \sum_{j=1}^{N} \int_{I_j} f'(u)\xi\xi_x \mathrm{d}x + \sum_{j=1}^{N} \left(\widehat{f'\xi}^{\,\mathrm{lin}} [\![\xi]\!]\right)_{j+\frac{1}{2}}\\
&= \sum_{j=1}^{N} \left( -\frac{1}{2}\int_{I_j} \partial_x f'(u)\xi^2 \mathrm{d}x - \left(f'(u)\{\!\{\xi\}\!\}[\![\xi]\!]\right)_{j+\frac{1}{2}} \right)\\
&\quad + \sum_{j=1}^{N} \left( \left( \left(\frac{1}{2}+\theta\right) f'(u) + \lambda\alpha \right) \xi^- + \left( \left(\frac{1}{2}-\theta\right) f'(u) - \lambda\alpha \right) \xi^+ \right)_{j+\frac{1}{2}} [\![\xi]\!]_{j+\frac{1}{2}}\\
&= \sum_{j=1}^{N} \left( -\frac{1}{2}\int_{I_j} \partial_x f'(u)\xi^2 \mathrm{d}x \right) - \sum_{j=1}^{N} (\theta f'(u) + \lambda\alpha)_{j+\frac{1}{2}} [\![\xi]\!]^2_{j+\frac{1}{2}}\\
&\le C\|\xi\|^2_{L^2(I)} + Z, \qquad (3.17)
\end{aligned}
$$

where

$$
Z = -\sum_{j=1}^{N} \left(\theta f'(u) + \lambda\alpha\right)_{j+\frac{1}{2}} [\![\xi]\!]^2_{j+\frac{1}{2}}. \tag{3.18}
$$

To estimate $Z$, let us split the sum with respect to $j$ into three parts based on values of $|f'(u_{j+\frac{1}{2}})|$, namely for a given constant $\tilde{C} = \lambda C/(\lambda - |\theta|) > 0$ with $C$ satisfying $|\varepsilon| \le Ch$

$$
Z = Z_1 + Z_2 + Z_3, \tag{3.19}
$$

where

$$
\begin{aligned}
Z_1 &= -\sum_{f'(u_{j+\frac{1}{2}})=0} \left(\theta f'(u) + \lambda\alpha\right)_{j+\frac{1}{2}} [\![\xi]\!]^2_{j+\frac{1}{2}},\\
Z_2 &= -\sum_{|f'(u_{j+\frac{1}{2}})|\le \tilde{C}h} \left(\theta f'(u) + \lambda\alpha\right)_{j+\frac{1}{2}} [\![\xi]\!]^2_{j+\frac{1}{2}},\\
Z_3 &= -\sum_{|f'(u_{j+\frac{1}{2}})| > \tilde{C}h} \left(\theta f'(u) + \lambda\alpha\right)_{j+\frac{1}{2}} [\![\xi]\!]^2_{j+\frac{1}{2}}.
\end{aligned}
$$

For $Z_1$, it is easy to show that

$$
Z_1 = -\sum_{f'(u_{j+\frac{1}{2}})=0} \lambda\alpha_{j+\frac{1}{2}} [\![\xi]\!]^2_{j+\frac{1}{2}} \le 0. \tag{3.20a}
$$

For the index set satisfying $|f'(u_{j+\frac{1}{2}})| \le \tilde{C}h$, by (3.13), we have

$$
|\theta f'(u_{j+\frac{1}{2}}) + \lambda\alpha_{j+\frac{1}{2}}| \le Ch.
$$

Then, by the inverse property (ii), we get

$$
Z_2 \le Ch\|\xi\|^2_{L^2(\Gamma_h)} \le C\|\xi\|^2_{L^2(I)}. \tag{3.20b}
$$

As to the index set satisfying $|f'(u_{j+\frac{1}{2}})| > \tilde{C}h$, by (3.13) and the choice of $\tilde{C}$, we deduce that

$$\theta f'(u_{j+\frac{1}{2}}) + \lambda\alpha_{j+\frac{1}{2}} \geq (\lambda - |\theta|)|f'(u_{j+\frac{1}{2}})| - \lambda|\varepsilon| \geq 0,$$

since $|\varepsilon| \leq Ch$. Thus

$$Z_3 \leq 0. \tag{3.20c}$$

Substituting (3.20a)–(3.20c) into (3.17), we arrive at the estimate of $\xi$ terms,

$$\mathcal{H}(f'(u)\xi, \xi; \widehat{f'\xi}^{\,\mathrm{lin}}) \leq C\|\xi\|^2_{L^2(I)}, \tag{3.21}$$

where $C$ is independent of $h$.

*Remark* 3.4. We can see that the condition (2.2b), namely $\lambda > |\theta|$, is crucial for the estimate of $\mathcal{H}(f'(u)\xi, \xi; \widehat{f'\xi}^{\,\mathrm{lin}})$, especially in driving (3.20c). Moreover, the nonnegative number $\theta f'(u_{j+\frac{1}{2}}) + \lambda\alpha_{j+\frac{1}{2}}$ can be regarded as the numerical viscosity coefficient for the GLLF fluxes (2.2), which allows us to choose suitable $\lambda$ and $\theta$ (closer $\lambda$ and $|\theta|$) such that the numerical viscosity coefficient is smaller than that of purely upwind fluxes. This is useful for resolving shocks even without nonlinear limiters; see, e.g., Figures 1 and 2 below.

**Step 4: Estimate of higher order terms.** For higher order terms, it follows from the Cauchy–Schwarz inequality, the inverse properties (i)–(iii), and the optimal approximation property (3.2) that

$$\begin{aligned}
\mathcal{H}(R_0e^2, \xi; \widehat{Re^2}^{\,\mathrm{nlr}}) &\leq \sum_{j=1}^{N} \left| \int_{I_j} R_0 e^2 \xi_x \mathrm{d}x + \big(\widehat{Re^2}^{\,\mathrm{nlr}} [\![\xi]\!]\big)_{j+\frac{1}{2}} \right| \\
&\leq C\|e\|_{L^\infty(I)}\big(\|e\|_{L^2(I)}\|\xi_x\|_{L^2(I)} + \|e\|_{L^2(\Gamma_h)}\|\xi\|_{L^2(\Gamma_h)}\big) \\
&\leq Ch^{-1}\|e\|_{L^\infty(I)}\big(\|\eta\|_{L^2(I)} + \|\xi\|_{L^2(I)} + h^{\frac{1}{2}}\|\eta\|_{L^2(\Gamma_h)}\big)\|\xi\|_{L^2(I)} \\
&\leq Ch^{-1}\|e\|_{L^\infty(I)}\big(\|\xi\|_{L^2(I)} + h^{k+1}\big)\|\xi\|_{L^2(I)},
\end{aligned}$$

which, by (3.5) implied by the a priori assumption (3.4), is

$$\mathcal{H}(R_0e^2, \xi; \widehat{Re^2}^{\,\mathrm{nlr}}) \leq C\|\xi\|^2_{L^2(I)} + Ch^{k+1}\|\xi\|_{L^2(I)}, \tag{3.22}$$

where $C$ is independent of $h$.

**Step 5: The final estimate of $\|\xi\|_{L^2(I)}$.** Collecting the estimates (3.16), (3.21), and (3.22) into (3.9) and using the Cauchy–Schwarz inequality, we arrive at the following inequality for $\|\xi\|_{L^2(I)}$:

$$\frac{1}{2}\frac{\mathrm{d}}{\mathrm{d}t}\|\xi\|^2_{L^2(I)} \leq \|\eta_t\|_{L^2(I)}\|\xi\|_{L^2(I)} + C\|\xi\|^2_{L^2(I)} + Ch^{k+1}\|\xi\|_{L^2(I)}. \tag{3.23}$$

By the definition of $\mathcal{P}_h$ in (3.1), we can see that $\mathcal{P}_h$ depends solely on $u$ and two constants $\lambda, \theta$, indicating that $\mathcal{P}_h$ is a linear operator of $u$. Indeed, this can be seen clearly from the explicit formula of $\mathcal{P}_h$ depending only on the integrals and point values of $u$, following the argument in [17, section 4.1]. Thus, $\eta_t = u_t - (\mathcal{P}_h u)_t = u_t - \mathcal{P}_h(u_t)$. Therefore, by Lemma 3.2

$$\|\eta_t\|_{L^2(I)} \leq Ch^{k+1}\|u_t\|_{H^{k+1}(\mathcal{I}_h)}.$$

Substituting the above estimate into (3.23) and using Young's inequality, one has

$$\frac{1}{2}\frac{\mathrm{d}}{\mathrm{d}t}\|\xi\|^2_{L^2(I)} \le C\|\xi\|^2_{L^2(I)} + Ch^{2k+2}.$$

Application of Gronwall's inequality together with initial error estimate (3.3) leads to

$$\|\xi(t)\|_{L^2(I)} \le Ch^{k+1} \quad \forall t \in (0,T], \tag{3.24}$$

where $C$ is independent of $h$. The optimal error estimate (3.6) in Theorem 3.3 can thus be obtained by taking into account $\|\eta(t)\|_{L^2(I)} \le Ch^{k+1}$.

*Remark* 3.5. For the Dirichlet boundary conditions, the optimal error estimates conclusion of Theorem 3.3 is still valid. The Dirichlet boundary conditions have two cases that the signs of $f'(u)$ at two end boundaries of $I$ are the same or different. For such cases, numerical fluxes at $x_{1/2}$ and $x_{N+1/2}$ should be chosen as (3.25) or (3.26) of [17, section 3.5], respectively. As to the design and analysis for projections, following [17, 20], for the projection errors we can require an exact collocation at the outflow boundary while asking for another collocation with weights $\lambda, \theta$ on which $f'(u_{j+1/2})$ is sign definite. This yields a *piecewise global* projection similar to that in (3.1). The optimal error estimates can be obtained analogously, and a detailed proof is omitted.

**4. Numerical experiments.** In this section, we present some numerical examples mainly addressing the following two issues. One is the sharpness of optimal error estimates in Theorem 3.3, which hold not only for *monotone* GLLF fluxes under condition (2.3) but also for the GLLF flux that is not *monotone* when some suitable weights are chosen. Another issue is the excellent performance of GLLF fluxes in resolving shocks, especially for those which are not *monotone*.

For all examples, the third order TVD Runge–Kutta time discretization is used with some suitable time steps. In Examples 4.1 and 4.2, $\tau = CFL_k \cdot h^{r_k}$ for $P^k$ $(1 \le k \le 4)$ polynomials with $r_1 = r_2 = 1$, $r_3 = 1.334 > 4/3$, $r_4 = 1.667 > 5/3$ and $CFL_1 = 0.1$, $CFL_2 = CFL_3 = CFL_4 = 0.05$. Uniform meshes are used.

*Example* 4.1. Consider the Burgers equation

$$\begin{cases} u_t + \left(\dfrac{u^2}{2}\right)_x = 0, & (x,t) \in [-1,1] \times (0,T], \\ u(x,0) = u_0(x), & x \in [-1,1], \end{cases}$$

with periodic boundary conditions, where $u_0(x) = \frac{1}{2}\sin(\pi x) + \frac{1}{4}$ for $x \in [-1,1]$.

The numerical errors and orders for different weights at $T = 0.3$ for which the exact is still smooth are listed in Table 1. From the table, we conclude that optimal orders of $k+1$ can always be observed for GLLF fluxes, no matter whether it is *monotone* or not.

To demonstrate stability and especially for *nonmonotone* GLLF fluxes, we consider Example 4.1 with $T = 12$ that a shock has been developed. The cell averages of DG solutions at $T = 12$ with 80 cells are shown in Figure 1, from which we can see that the DG scheme with GLLF fluxes is always stable with potential advantages in resolving shocks; see subfigure (e). In Figure 2, we plot the pointwise values of DG solutions for the cells from No. 33 to No. 40 among the total 80 cells. It seems that the numerical solution for the weights in subfigure (f) is less oscillatory than that of the standard LLF flux in subfigure (b), especially for $P^1$ elements.

TABLE 1
*$L^2$ errors and orders for Example 4.1 using $P^k$ polynomials with different $\lambda$, $\theta$ on uniform mesh of $N$ cells. $T = 0.3$.*

| | $N$ | $\lambda = 0.5$, $\theta = -0.25$ | | $\lambda = 0.5$, $\theta = 0$ | | $\lambda = 0.5$, $\theta = 0.25$ | | $\lambda = 1.25$, $\theta = 0$ | |
|---|---|---|---|---|---|---|---|---|---|
| | | $L^2$ error | Order | $L^2$ error | Order | $L^2$ error | Order | $L^2$ error | Order |
| $P^1$ | 20 | 4.92E-03 | – | 3.96E-03 | – | 4.20E-03 | – | 3.21E-03 | – |
| | 40 | 1.37E-03 | 1.84 | 1.05E-03 | 1.91 | 1.17E-03 | 1.84 | 8.04E-03 | 2.00 |
| | 80 | 3.70E-04 | 1.89 | 2.75E-04 | 1.94 | 3.17E-04 | 1.89 | 2.02E-04 | 1.99 |
| | 160 | 9.71E-05 | 1.93 | 7.10E-05 | 1.96 | 8.35E-05 | 1.92 | 5.09E-05 | 1.99 |
| $P^2$ | 20 | 2.40E-04 | – | 2.49E-04 | – | 2.63E-04 | – | 3.01E-04 | – |
| | 40 | 3.00E-05 | 3.00 | 3.38E-05 | 2.88 | 3.82E-05 | 2.78 | 4.81E-05 | 2.65 |
| | 80 | 3.83E-06 | 2.97 | 4.52E-06 | 2.90 | 5.37E-06 | 2.83 | 7.34E-06 | 2.71 |
| | 160 | 4.86E-07 | 2.98 | 5.89E-07 | 2.94 | 7.24E-07 | 2.89 | 1.05E-06 | 2.81 |
| $P^3$ | 20 | 2.07E-05 | – | 1.96E-05 | – | 1.98E-05 | – | 2.00E-05 | – |
| | 40 | 1.64E-06 | 3.66 | 1.40E-06 | 3.91 | 1.34E-06 | 3.88 | 1.28E-06 | 3.97 |
| | 80 | 1.23E-07 | 3.74 | 9.38E-08 | 3.90 | 8.64E-08 | 3.96 | 7.72E-08 | 4.05 |
| | 160 | 8.70E-09 | 3.82 | 6.15E-09 | 3.93 | 5.61E-09 | 3.95 | 4.82E-09 | 4.00 |
| $P^4$ | 20 | 2.45E-06 | – | 2.17E-06 | – | 2.09E-06 | – | 2.08E-06 | – |
| | 40 | 7.02E-08 | 5.12 | 7.25E-08 | 4.90 | 7.63E-08 | 4.78 | 8.52E-08 | 4.61 |
| | 80 | 2.14E-09 | 5.04 | 2.44E-09 | 4.89 | 2.78E-09 | 4.78 | 3.49E-09 | 4.61 |
| | 160 | 6.72E-11 | 4.99 | 7.97E-11 | 4.93 | 9.55E-11 | 4.86 | 1.32E-10 | 4.73 |

In order to show long time behavior of DG errors for GLLF fluxes, in what follows we consider two nonhomogeneous nonlinear hyperbolic equations with smooth exact solution. Note that the optimal error estimates may not be valid for such an equation. This is because the proposed special projection $\mathcal{P}_h$ does not work, as the characteristic lines may be curved and thus the zeros of $f'(u(x,t))$ can be dependent on $t$.

*Example* 4.2. Consider the following nonhomogeneous nonlinear equation:

$$\begin{cases} u_t + \left(\dfrac{u^2}{2}\right)_x = g(x,t), & (x,t) \in [0, 2\pi] \times (0, T], \\ u(x,0) = u_0(x), & x \in [0, 2\pi], \end{cases}$$

with periodic boundary conditions, where $u_0(x) = \sin x$, $g(x,t) = \frac{1}{2}\sin(2x - t)$ such that the exact solution is $u(x,t) = \sin(x - \frac{t}{2}) + \frac{1}{2}$.

The $L^2$ numerical errors and orders with different $\lambda, \theta$ at $T = \pi$ are given in Table 2, from which we conclude that the DG scheme (2.1) with GLLF fluxes for the nonlinear equation in Example 4.2 also achieves optimal $(k+1)$th order of accuracy. Moreover, when the final time $T$ is large enough, the errors do not show growth; for instance, when $T = 100$, $N = 160$, $(\lambda, \theta) = (0.5, -0.25)$, the $L^2$ errors are still 4.72E-07 for the $P^2$ case.

*Example* 4.3. Consider the following equation with strong nonlinearity:

$$\begin{cases} u_t + \left(e^u\right)_x = g(x,t), & (x,t) \in [0, 2\pi] \times (0, T], \\ u(x,0) = u_0(x), & x \in [0, 2\pi], \end{cases}$$

with periodic boundary conditions, where $u_0(x) = \sin x$, $g(x,t) = \cos(x-t)(e^{\sin(x-t)} - 1)$ such that the exact solution is $u(x,t) = \sin(x - t)$.

In this example, we only present numerical results for the $P^2$ and $P^3$ cases, and $\tau = CFL_k \cdot h^{r_k}$ for $P^k$ $(k = 2, 3)$ polynomials with $r_2 = 1$, $r_3 = 1.334 > 4/3$ and

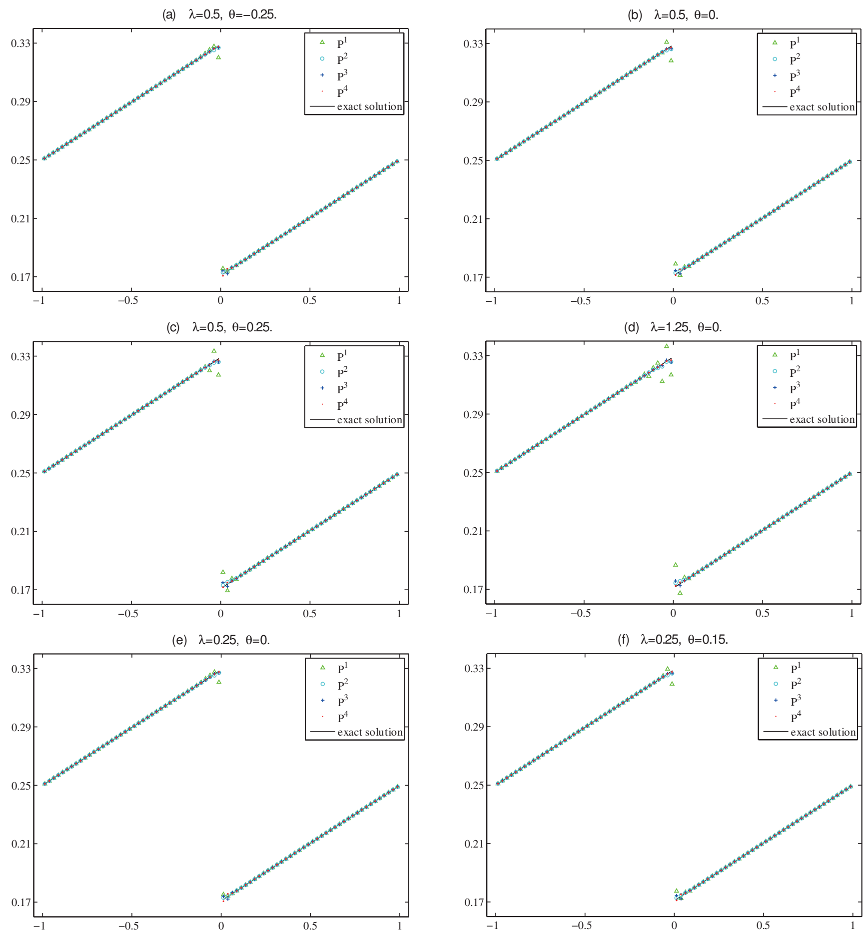


FIG. 1. *Cell averages of DG solutions in Example* 4.1 *using* $P^k$ *polynomials.* $N = 80$, $T = 12$.

$CFL_2 = CFL_3 = 0.03$. The $L^2$ errors and orders with different $\lambda, \theta$ at $T = \pi$ are given in Table 3, from which we can also observe the expected optimal $(k+1)$th order of accuracy for the DG error.

Numerical results of Examples 4.2 and 4.3 indicate that the DG scheme with GLLF fluxes maintains stability and exhibits excellent long time behaviors, even for conservation laws with strong nonlinearity. In addition, it seems that the DG scheme with smaller numerical viscosity coefficients (closer $\lambda$ and $|\theta|$) produces smaller magnitude of DG errors for even $k$, while it produces bigger magnitude of DG errors for odd $k$. This agrees with numerical results for the linear version of GLLF fluxes in [20], in which linear hyperbolic equations with upwind-biased fluxes are considered.

**5. Concluding remarks.** In this paper, we study the DG scheme with GLLF fluxes for scalar nonlinear conservation laws. The stability of the DG scheme is established when $\lambda \geq \frac{1}{2} + |\theta|$, and optimal a priori error estimates are obtained under the condition $\lambda > |\theta|$, for which linear stability can be proved [20]. The main technicality is the construction and analysis of a *piecewise global* projection, which not only eliminates as many projection error terms as possible with provable optimal

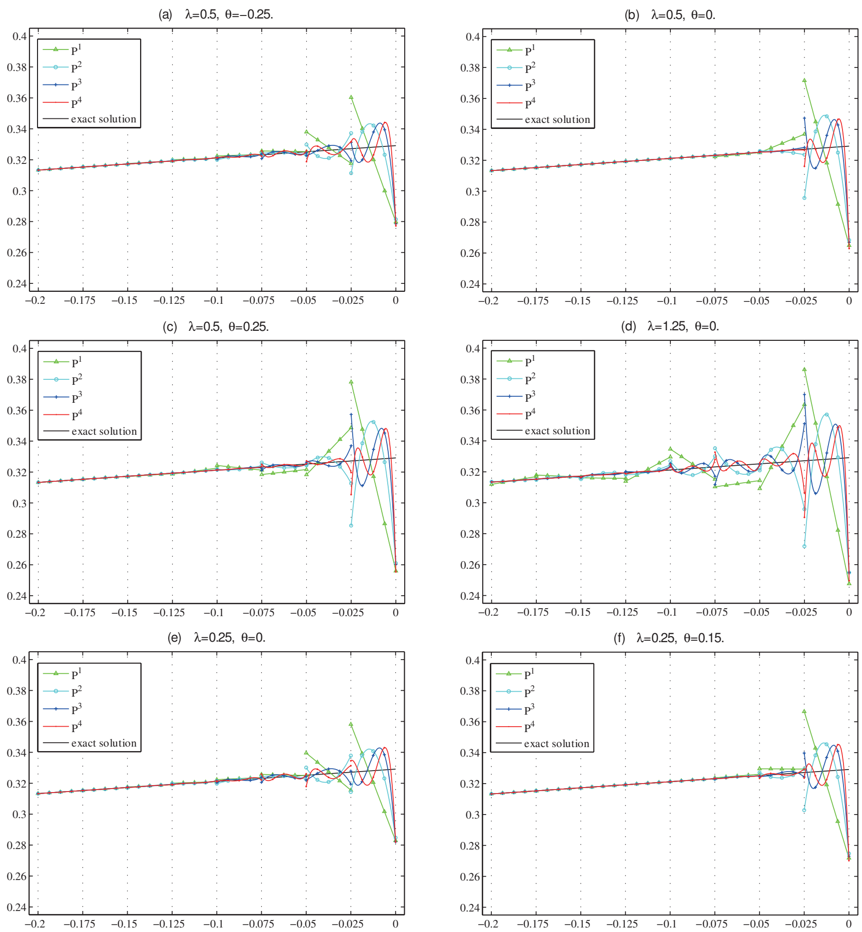


FIG. 2. *Pointwise values of DG solutions in Example* 4.1 *using* $P^k$ *polynomials.* $N = 80$, $T = 12$.

approximation property, but also commutes with the time derivative operator. It is worth pointing out that the optimal error estimates are also valid for GLLF fluxes that are not *monotone*, and the numerical viscosity coefficients are adjustable, making it possible to better resolve shocks. Numerical experiments are given to validate the theoretical results. Future work includes a rigorous study of stability for *non-monotone* GLLF fluxes with $|\theta| < \lambda < |\theta| + \frac{1}{2}$ and extension to two-dimensional nonlinear conservation laws.

**Appendix A. Proof of Lemma 3.2.** First, let us introduce the standard locally defined GR projection $P_h^-$, whose definition is as follows. For $u \in H^1(\mathcal{I}_h)$, $P_h^- u \in V_h^k$ is the unique piecewise polynomial satisfying

$$\int_{I_j} (P_h^- u)\varphi \mathrm{d}x = \int_{I_j} u\varphi \mathrm{d}x \quad \forall \varphi \in P^{k-1}(I_j), \tag{A.1a}$$

$$(\mathcal{P}_h u)^-_{j+\frac{1}{2}} = u^-_{j+\frac{1}{2}} \qquad \text{at } x_{j+\frac{1}{2}} \tag{A.1b}$$

TABLE 2

*$L^2$ errors and orders for Example 4.2 using $P^k$ polynomials with different $\lambda$, $\theta$ on uniform mesh of $N$ cells. $T = \pi$.*

| | $N$ | $\lambda = 0.5$, $\theta = -0.25$ | | $\lambda = 0.5$, $\theta = 0$ | | $\lambda = 0.5$, $\theta = 0.25$ | | $\lambda = 1.25$, $\theta = 0$ | |
|---|---|---|---|---|---|---|---|---|---|
| | | $L^2$ error | Order | $L^2$ error | Order | $L^2$ error | Order | $L^2$ error | Order |
| $P^1$ | 20 | 1.44E-02 | – | 1.08E-02 | – | 1.33E-02 | – | 7.05E-03 | – |
| | 40 | 3.60E-03 | 2.00 | 2.67E-03 | 2.02 | 3.39E-03 | 1.98 | 1.84E-03 | 2.02 |
| | 80 | 8.97E-04 | 2.01 | 6.64E-04 | 2.01 | 8.56E-04 | 1.98 | 4.59E-04 | 2.01 |
| | 160 | 2.24E-04 | 2.00 | 1.66E-04 | 2.00 | 2.15E-04 | 1.99 | 1.15E-04 | 2.00 |
| $P^2$ | 20 | 2.60E-04 | – | 3.25E-04 | – | 4.17E-04 | – | 6.92E-04 | – |
| | 40 | 3.32E-05 | 2.97 | 3.83E-05 | 3.08 | 4.75E-05 | 3.13 | 8.43E-05 | 3.04 |
| | 80 | 3.91E-06 | 3.09 | 4.46E-06 | 3.10 | 5.50E-06 | 3.11 | 9.27E-06 | 3.18 |
| | 160 | 4.72E-07 | 3.05 | 5.37E-07 | 3.05 | 6.64E-07 | 3.05 | 1.07E-06 | 3.11 |
| $P^3$ | 20 | 6.72E-06 | – | 5.32E-06 | – | 6.98E-06 | – | 3.88E-06 | – |
| | 40 | 4.29E-07 | 3.97 | 3.30E-07 | 4.01 | 4.17E-07 | 4.06 | 2.38E-07 | 4.02 |
| | 80 | 2.72E-08 | 3.98 | 2.07E-08 | 3.99 | 2.63E-08 | 3.99 | 1.48E-08 | 4.00 |
| | 160 | 1.70E-09 | 4.00 | 1.29E-09 | 4.00 | 1.64E-09 | 4.00 | 9.26E-10 | 4.00 |
| $P^4$ | 20 | 1.19E-07 | – | 1.31E-07 | – | 1.56E-07 | – | 2.50E-07 | – |
| | 40 | 3.74E-09 | 5.00 | 4.00E-09 | 5.03 | 4.52E-09 | 5.11 | 7.15E-09 | 5.13 |
| | 80 | 1.15E-10 | 5.02 | 1.22E-10 | 5.04 | 1.36E-10 | 5.06 | 1.99E-10 | 5.17 |
| | 160 | 3.55E-12 | 5.02 | 3.75E-12 | 5.02 | 4.15E-12 | 5.03 | 5.83E-12 | 5.09 |

TABLE 3

*$L^2$ errors and orders for Example 4.3 using $P^k$ polynomials with different $\lambda$, $\theta$ on uniform mesh of $N$ cells. $T = \pi$.*

| | $N$ | $\lambda = 0.5$, $\theta = -0.25$ | | $\lambda = 0.5$, $\theta = 0$ | | $\lambda = 0.5$, $\theta = 0.25$ | | $\lambda = 1.25$, $\theta = 0$ | |
|---|---|---|---|---|---|---|---|---|---|
| | | $L^2$ error | Order | $L^2$ error | Order | $L^2$ error | Order | $L^2$ error | Order |
| $P^2$ | 20 | 2.04E-04 | – | 2.70E-04 | – | 3.50E-04 | – | 5.12E-04 | – |
| | 40 | 2.52E-05 | 3.02 | 3.36E-05 | 3.01 | 4.40E-05 | 2.99 | 6.66E-05 | 2.94 |
| | 80 | 3.14E-06 | 3.00 | 4.19E-06 | 3.00 | 5.51E-06 | 3.00 | 8.42E-06 | 2.98 |
| | 160 | 3.93E-07 | 3.00 | 5.24E-07 | 3.00 | 6.89E-07 | 3.00 | 1.05E-06 | 3.00 |
| $P^3$ | 20 | 8.15E-06 | – | 5.22E-06 | – | 4.36E-06 | – | 3.83E-06 | – |
| | 40 | 5.26E-07 | 3.95 | 3.25E-07 | 4.01 | 2.70E-07 | 4.01 | 2.37E-07 | 4.01 |
| | 80 | 3.31E-08 | 3.99 | 2.03E-08 | 4.00 | 1.69E-08 | 3.00 | 1.48E-08 | 4.00 |
| | 160 | 2.07E-09 | 4.00 | 1.27E-09 | 4.00 | 1.05E-09 | 4.00 | 9.23E-10 | 4.00 |

for $j = 1, \ldots, N$. By the Bramble–Hilbert lemma and scaling arguments [3, 11], if $u \in H^{k+1}(\mathcal{I}_h)$, then there holds the following optimal approximation property:

$$\|u - P_h^- u\|_{L^2(I)} + h^{\frac{1}{2}} \|u - P_h^- u\|_{L^2(\Gamma_h)} \le C h^{k+1} \|u\|_{H^{k+1}(\mathcal{I}_h)}, \tag{A.2}$$

where $C$ is independent of $h$.

Then we prove the unique existence of $\mathcal{P}_h u$. By denoting $\mathcal{E} = \mathcal{P}_h u - P_h^- u$, $\psi = u - P_h^- u$, one has $\mathcal{P}_h u - u = \mathcal{E} - \psi$. The unique existence of $\mathcal{P}_h u$ can thus be obtained if we can prove existence of $\mathcal{E}$, since $\mathcal{P}_h u = \mathcal{E} + P_h^- u$. Denote by $\mathcal{E}_j$ the restriction of $\mathcal{E}$ on each $I_j$; then

$$\mathcal{E}_j(x) = \sum_{\ell=0}^{k} \alpha_{j,\ell} P_{j,\ell}(x) = \sum_{\ell=0}^{k} \alpha_{j,\ell} P_\ell(s), \quad j \in \mathbb{Z}_N^+, \tag{A.3}$$

where $P_\ell(s)$ is the $\ell$th order standard Legendre polynomial on $[-1, 1]$ with $s = \frac{2(x - x_j)}{h_j}$ and $P_{j,\ell}(x)$ is the scaled Legendre polynomial on $I_j$.

From (3.1a) and (A.1a), there holds $\int_{I_j} \mathcal{E}\varphi \mathrm{d}x = 0\ \forall \varphi \in P^{k-1}(I_j),\ j \in \mathbb{Z}_N^+$. Then, due to the orthogonality properties of the Legendre polynomials, we obtain

$$\alpha_{j,\ell} = 0, \quad \ell = 0, \dots, k-1,\ j \in \mathbb{Z}_N^+.$$

Hence, we have $\mathcal{E}_j(x) = \alpha_{j,k} P_k(s)$. Noting that analysis of $\alpha_{j,k}$ is the key factor to unique existence, we thus consider $\alpha_{j,k}$ when $j$ is taken as different values, which are divided into the following three cases.

When $j = \gamma$, we can easily obtain that $\mathcal{E}_j(x^-_{\gamma+\frac{1}{2}}) = 0$ by (3.1b) and (A.1b), which yields $\alpha_{\gamma,k} = 0$.

When $j \in \mathbb{b}^+$, by (3.1c) and (A.1b), one has

$$\widehat{\mathcal{E}}^p_{j+\frac{1}{2}} = \left(\frac{1}{2} - (\lambda+\theta)\right) \psi^+_{j+\frac{1}{2}} \quad \forall j \in \mathbb{b}^+,$$

which implies

$$\left(\frac{1}{2} + (\lambda+\theta)\right) \alpha_{j,k} + \left(\frac{1}{2} - (\lambda+\theta)\right) (-1)^k \alpha_{j+1,k} = \left(\frac{1}{2} - (\lambda+\theta)\right) \psi^+_{j+\frac{1}{2}}, \quad j \in \mathbb{b}^+. \tag{A.4}$$

We see that the above system can be decoupled starting from the cell $I_\gamma$ by letting $j = \gamma - 1$ and using $\alpha_{\gamma,k} = 0$. Moreover, it can be written into the form

$$\mathbb{A}_{\mathbb{b}^+} \alpha_{\mathbb{b}^+} = \Theta_{\mathbb{b}^+} \psi_{\mathbb{b}^+},$$

where the vectors $\alpha_{\mathbb{b}^+} = (\alpha_{\beta,k}, \dots, \alpha_{\gamma-1,k})^\top$, $\psi_{\mathbb{b}^+} = (\psi^+_{\beta+\frac{1}{2}}, \dots, \psi^+_{\gamma-\frac{1}{2}})^\top$, the diagonal matrix $\Theta_{\mathbb{b}^+} = \mathrm{diag}\big(\frac{1}{2} - (\lambda+\theta), \dots, \frac{1}{2} - (\lambda+\theta)\big)$ is of size $|\mathbb{b}^+| \times |\mathbb{b}^+|$, and the upper triangular matrix

$$\mathbb{A}_{\mathbb{b}^+} = \begin{pmatrix} \frac{1}{2}+(\lambda+\theta) & (\frac{1}{2}-(\lambda+\theta))(-1)^k & & \\ & \ddots & \ddots & \\ & & \frac{1}{2}+(\lambda+\theta) & (\frac{1}{2}-(\lambda+\theta))(-1)^k \\ & & & \frac{1}{2}+(\lambda+\theta) \end{pmatrix}$$

is also of size $|\mathbb{b}^+| \times |\mathbb{b}^+|$.

When $j \in \mathbb{b}^-$, by (3.1d) and (A.1b), one has

$$\widehat{\mathcal{E}}^n_{j-\frac{1}{2}} = \left(\frac{1}{2} + (\lambda-\theta)\right) \psi^+_{j-\frac{1}{2}} \quad \forall j \in \mathbb{b}^-,$$

which implies

$$\left(\frac{1}{2} - (\lambda-\theta)\right) \alpha_{j-1,k} + \left(\frac{1}{2} + (\lambda-\theta)\right) (-1)^k \alpha_{j,k} = \left(\frac{1}{2} + (\lambda-\theta)\right) \psi^+_{j-\frac{1}{2}}, \quad j \in \mathbb{b}^-. \tag{A.5}$$

Similarly, $\alpha_{\gamma,k} = 0$ is still involved in (A.5), indicating that the above system can be decoupled starting from the cell $I_\gamma$ by letting $j = \gamma+1$ and using $\alpha_{\gamma,k} = 0$. Moreover, it can be written into the form

$$\mathbb{A}_{\mathbb{b}^-} \alpha_{\mathbb{b}^-} = \Theta_{\mathbb{b}^-} \psi_{\mathbb{b}^-},$$

where the vectors $\alpha_{\mathbb{b}^-} = (\alpha_{\gamma+1,k}, \ldots, \alpha_{\beta-1,k})^\top$, $\psi_{\mathbb{b}^-} = (\psi^+_{\gamma+\frac{1}{2}}, \ldots, \psi^+_{\beta-\frac{3}{2}})^\top$, the diagonal matrix $\Theta_{\mathbb{b}^-} = \mathrm{diag}(\frac{1}{2}+(\lambda-\theta), \ldots, \frac{1}{2}+(\lambda-\theta))$ is of size $|\mathbb{b}^-| \times |\mathbb{b}^-|$, and the lower triangular matrix

$$\mathbb{A}_{\mathbb{b}^-} = \begin{pmatrix} (\frac{1}{2}+(\lambda-\theta))(-1)^k & & & \\ \frac{1}{2}-(\lambda-\theta) & (\frac{1}{2}+(\lambda-\theta))(-1)^k & & \\ & \ddots & \ddots & \\ & & \frac{1}{2}-(\lambda-\theta) & (\frac{1}{2}+(\lambda-\theta))(-1)^k \end{pmatrix}$$

is also of size $|\mathbb{b}^-| \times |\mathbb{b}^-|$.

By the condition (2.2b), namely $\lambda > |\theta|$, we see that $\frac{1}{2} + (\lambda+\theta) \neq 0$ and $\big(\frac{1}{2} + (\lambda-\theta)\big)(-1)^k \neq 0$; then due to the special form of $\mathbb{A}_{\mathbb{b}^+}$ and $\mathbb{A}_{\mathbb{b}^-}$, we deduce that $|\mathbb{A}_{\mathbb{b}^+}| \neq 0$, $|\mathbb{A}_{\mathbb{b}^-}| \neq 0$, from which we can prove the unique existence of projection $\mathcal{P}_h u$.

In what follows let us prove the optimal approximation property of projection $\mathcal{P}_h u$. By denoting $\mathbb{M}_+ = \mathbb{A}^{-1}_{\mathbb{b}^+}\Theta_{\mathbb{b}^+}$ and $\mathbb{M}_- = \mathbb{A}^{-1}_{\mathbb{b}^-}\Theta_{\mathbb{b}^-}$, we find it is sufficient to prove that the matrix norms $\|\mathbb{M}_\pm\|_2$ are bounded. Here we pay attention to the fact that, when $\lambda > |\theta|$, there always holds

$$\left|\frac{\big(\frac{1}{2} - (\lambda+\theta)\big)(-1)^k}{\frac{1}{2} + (\lambda+\theta)}\right| < 1, \qquad \left|\frac{\frac{1}{2} - (\lambda-\theta)}{\big(\frac{1}{2} + (\lambda-\theta)\big)(-1)^k}\right| < 1,$$

which are involved in the entries of $\mathbb{M}_+$ and $\mathbb{M}_-$. Then we can obtain that $\|\mathbb{M}_\pm\|_2$ are bounded if we follow the same lines as that in the analysis of $\|\mathbb{M}_\pm\|_2$ in [17, Lemma 3.1]. Since there is no essential difference, we do not present a detailed proof to save space.

Consequently, by (A.2)

$$\begin{aligned}\|\alpha_{\mathbb{b}^+}\|_2^2 &= \|\mathbb{M}_+\psi_{\mathbb{b}^+}\|_2^2 \le \|\mathbb{M}_+\|_2^2 \cdot \|\psi_{\mathbb{b}^+}\|_2^2 \le C\|\psi_{\mathbb{b}^+}\|_2^2 \\ &\le C\|u - P_h^- u\|^2_{L^2(\Gamma_h)} \le Ch^{2k+1}\|u\|^2_{H^{k+1}(\mathcal{I}_h)}, \\ \|\alpha_{\mathbb{b}^-}\|_2^2 &= \|\mathbb{M}_-\psi_{\mathbb{b}^-}\|_2^2 \le \|\mathbb{M}_-\|_2^2 \cdot \|\psi_{\mathbb{b}^-}\|_2^2 \le C\|\psi_{\mathbb{b}^-}\|_2^2 \\ &\le C\|u - P_h^- u\|^2_{L^2(\Gamma_h)} \le Ch^{2k+1}\|u\|^2_{H^{k+1}(\mathcal{I}_h)}.\end{aligned}$$

By denoting $\alpha = (\alpha_{1,k}, \ldots, \alpha_{N,k})^\top$ and using $\alpha_{\gamma,k} = 0$, one has

$$\|\alpha\|_2^2 = \|\alpha_{\mathbb{b}^+}\|_2^2 + \|\alpha_{\mathbb{b}^-}\|_2^2 \le Ch^{2k+1}\|u\|^2_{H^{k+1}(\mathcal{I}_h)}, \tag{A.6}$$

since $\alpha_{\gamma,k} = 0$. Thus,

$$\begin{aligned}\|\mathcal{E}\|^2_{L^2(I)} &= \sum_{j=1}^N \alpha_{j,k}^2 \|P_{j,k}(x)\|^2_{L^2(I_j)} = \sum_{j=1}^N \frac{h_j\alpha_{j,k}^2}{2k+1} \le Ch\|\alpha\|_2^2, \\ \|\mathcal{E}\|^2_{L^2(\Gamma_h)} &= 2\sum_{j=1}^N \alpha_{j,k}^2 = 2\|\alpha\|_2^2,\end{aligned}$$

which, in combination with (A.6), gives us

$$\|\mathcal{E}\|_{L^2(I)} + h^{\frac{1}{2}}\|\mathcal{E}\|_{L^2(\Gamma_h)} \le Ch^{k+1}\|u\|_{H^{k+1}(\mathcal{I}_h)}, \tag{A.7}$$

where $C$ is independent of $h$. Then the optimal approximation property (3.2) for $\mathcal{P}_h u$ follows by combining (A.2) and (A.7).

## REFERENCES


[1] M. Ainsworth, P. Monk, and W. Muniz, *Dispersive and dissipative properties of discontinuous Galerkin finite element methods for the second-order wave equation*, J. Sci. Comput., 27 (2006), pp. 5–40.

[2] J. L. Bona, H. Chen, O. Karakashian, and Y. Xing, *Conservative, discontinuous Galerkin-methods for the generalized Korteweg–de Vries equation*, Math. Comp., 82 (2013), pp. 1401–1432.

[3] S. C. Brenner and L. R. Scott, *The Mathematical Theory of Finite Element Methods*, 3rd ed., Texts in Appl. Math. 15, Springer, New York, 2008.

[4] E. Burman, A. Ern, and M. A. Fernández, *Explicit Runge–Kutta schemes and finite elements with symmetric stabilization for first-order linear PDE systems*, SIAM J. Numer. Anal., 48 (2010), pp. 2019–2042.

[5] W. Cao, D. Li, Y. Yang, and Z. Zhang, *Superconvergence of discontinuous Galerkin methods based on upwind-biased fluxes for 1D linear hyperbolic equations*, ESAIM Math. Model. Numer. Anal., 51 (2017), pp. 467–486.

[6] P. Castillo, B. Cockburn, D. Schötzau, and C. Schwab, *Optimal a priori error estimates for the hp-version of the local discontinuous Galerkin method for convection-diffusion problems*, Math. Comp., 71 (2002), pp. 455–478.

[7] Z. Chen, H. Huang, and J. Yan, *Third order maximum-principle-satisfying direct discontinuous Galerkin methods for time dependent convection diffusion equations on unstructured triangular meshes*, J. Comput. Phys., 308 (2016), pp. 198–217.

[8] Y. Cheng, C.-S. Chou, F. Li, and Y. Xing, *$L^2$ stable discontinuous Galerkin methods for one-dimensional two-way wave equations*, Math. Comp., 86 (2017), pp. 121–155.

[9] Y. Cheng, X. Meng, and Q. Zhang, *Application of generalized Gauss–Radau projections for the local discontinuous Galerkin method for linear convection-diffusion equations*, Math. Comp., 86 (2017), pp. 1233–1267.

[10] Y. Cheng and Q. Zhang, *Local analysis of the local discontinuous Galerkin method with generalized alternating numerical flux for one-dimensional singularly perturbed problem*, J. Sci. Comput., 72 (2017), pp. 792–819.

[11] P. G. Ciarlet, *The Finite Element Method for Elliptic Problems*, Stud. Math. Appl. 4, North-Holland, Amsterdam, 1978.

[12] B. Cockburn and C.-W. Shu, *TVB Runge–Kutta local projection discontinuous Galerkin finite element method for conservation laws.* II. *General framework*, Math. Comp., 52 (1989), pp. 411–435.

[13] R. S. Falk and G. R. Richter, *Explicit finite element methods for symmetric hyperbolic equations*, SIAM J. Numer. Anal., 36 (1999), pp. 935–952.

[14] P. Fu, Y. Cheng, F. Li, and Y. Xu, *Discontinuous Galerkin methods with optimal $L^2$ accuracy for one dimensional linear PDEs with high order spatial derivatives*, J. Sci. Comput., 78 (2019), pp. 816–863.

[15] S. Gottlieb, C.-W. Shu, and E. Tadmor, *Strong stability-preserving high-order time discretization methods*, SIAM Rev., 43 (2001), pp. 89–112.

[16] G. S. Jiang and C.-W. Shu, *On a cell entropy inequality for discontinuous Galerkin methods*, Math. Comp., 62 (1994), pp. 531–538.

[17] J. Li, D. Zhang, X. Meng, and B. Wu, *Analysis of discontinuous Galerkin methods with upwind-biased fluxes for one dimensional linear hyperbolic equations with degenerate variable coefficients*, J. Sci. Comput., 78 (2019), pp. 1305–1328.

[18] H. Liu and N. Ploymaklam, *A local discontinuous Galerkin method for the Burgers–Poisson equation*, Numer. Math., 129 (2015), pp. 321–351.

[19] H. Liu and J. Yan, *The direct discontinuous Galerkin (DDG) methods for diffusion problems*, SIAM J. Numer. Anal., 47 (2009), pp. 675–698.

[20] X. Meng, C.-W. Shu, and B. Wu, *Optimal error estimates for discontinuous Galerkin methods based on upwind-biased fluxes for linear hyperbolic equations*, Math. Comp., 85 (2016), pp. 1225–1261.

[21] X. Meng, C.-W. Shu, Q. Zhang, and B. Wu, *Superconvergence of discontinuous Galerkin methods for scalar nonlinear conservation laws in one space dimension*, SIAM J. Numer. Anal., 50 (2012), pp. 2336–2356.

[22] S. Osher, *Riemann solvers, the entropy condition, and difference approximations*, SIAM J. Numer. Anal., 21 (1984), pp. 217–235.

[23] W. H. Reed and T. R. Hill, *Triangular Mesh Methods for the Neutron Transport Equation*, Technical report LA-UR-73-479, Los Alamos Scientific Laboratory, Los Alamos, NM, 1973.

[24] C.-W. Shu, *Discontinuous Galerkin methods: General approach and stability*, in Numerical Solutions of Partial Differential Equations, Adv. Courses Math. CRM Barcelona, Birkhäuser, Basel, 2009, pp. 149–201.

[25] C.-W. Shu, *Discontinuous Galerkin method for time-dependent problems: Survey and recent developments*, in Recent Developments in Discontinuous Galerkin Finite Element Methods for Partial Differential Equations, IMA Vol. Math. Appl. 157, Springer, Cham, 2014, pp. 25–62.

[26] Q. Zhang and C.-W. Shu, *Stability analysis and a priori error estimates of the third order explicit Runge–Kutta discontinuous Galerkin method for scalar conservation laws*, SIAM J. Numer. Anal., 48 (2010), pp. 1038–1063.